Single-Junction Binary-Blend Nonfullerene Polymer Solar Cells with 12.1% Efficiency

Fuwen Zhao, Shuixing Dai, Yang Wu, Qianqian Zhang, Jiayu Wang, Li Jiang, Qidan Ling, Zhixiang Wei, Wei Ma, Wei You, Chunru Wang, and Xiaowei Zhan**

A new fluorinated nonfullerene acceptor, ITIC-Th1, has been designed and synthesized by introducing fluorine (F) atoms onto the end-capping group 1,1-dicyanomethylene-3-indanone (IC). On the one hand, incorporation of F would improve intramolecular interaction, enhance the push–pull effect between the donor unit indacenodithieno[3,2-b]thiophene and the acceptor unit IC due to electron-withdrawing effect of F, and finally adjust energy levels and reduce bandgap, which is beneficial to light harvesting and enhancing short-circuit current density (J_{SC}). On the other hand, incorporation of F would improve intermolecular interactions through C—F···S, C—F···H, and C—F···π noncovalent interactions and enhance electron mobility, which is beneficial to enhancing J_{SC} and fill factor. Indeed, the results show that fluorinated ITIC-Th1 exhibits redshifted absorption, smaller optical bandgap, and higher electron mobility than the nonfluorinated ITIC-Th. Furthermore, nonfullerene organic solar cells (OSCs) based on fluorinated ITIC-Th1 electron acceptor and a wide-bandgap polymer donor FTAZ based on benzodithiophene and benzotriazole exhibit power conversion efficiency (PCE) as high as 12.1%, significantly higher than that of nonfluorinated ITIC-Th (8.88%). The PCE of 12.1% is the highest in fullerene and nonfullerene-based single-junction binary-blend OSCs. Moreover, the OSCs based on FTAZ:ITIC-Th1 show much better efficiency and better stability than the control devices based on FTAZ:$PC_{71}BM$ (PCE = 5.22%).

As a promising technology for clean and renewable energy conversion, organic solar cells (OSCs) have attracted considerable attention in recent years since they have a number of attractive features, such as low cost, light weight, flexibility, and semi-transparency.[1–6] Fullerene derivatives (e.g., $PC_{61}BM$ and $PC_{71}BM$) are the classical electron acceptors in OSCs during the last two decades and they exhibit high electron affinity and isotropic charge transport with good mobility, due to unique spherical geometry.[7,8] The power conversion efficiency (PCE) over 11% has been achieved for fullerene-based OSCs;[9,10] however, its weak absorption in the visible region and limited tunability in energy levels restrict further development of the OSCs.

Nonfullerene acceptors, as the alternative to fullerene acceptors, attracted increasing attention in recent years, because they present good light harvesting capability and facile energy level modulation, which are beneficial to achieving high short-circuit current density (J_{SC}) and high

F. Zhao, S. Dai, J. Wang, Prof. X. Zhan
Department of Materials Science and Engineering
College of Engineering
Key Laboratory of Polymer Chemistry and Physics
of Ministry of Education
Peking University
Beijing 100871, China
E-mail: xwzhan@pku.edu.cn

F. Zhao, Dr. L. Jiang, Prof. C. Wang
Institute of Chemistry
Chinese Academy of Sciences
Beijing 100190, China
E-mail: crwang@iccas.ac.cn

S. Dai, Prof. Q. Ling
Fujian Key Laboratory of Polymer Materials
College of Materials Science and Engineering
Fujian Normal University
Fuzhou 350007, China

Y. Wu, Prof. W. Ma
State Key Laboratory for Mechanical Behavior
of Materials
Xi'an Jiaotong University
Xi'an 710049, China

Q. Zhang, Prof. W. You
Department of Chemistry
University of North Carolina at Chapel Hill
Chapel Hill, NC 27599-3290, USA

Prof. Z. Wei
National Center for Nanoscience and Technology
Beijing 100190, China

DOI: 10.1002/adma.201700144

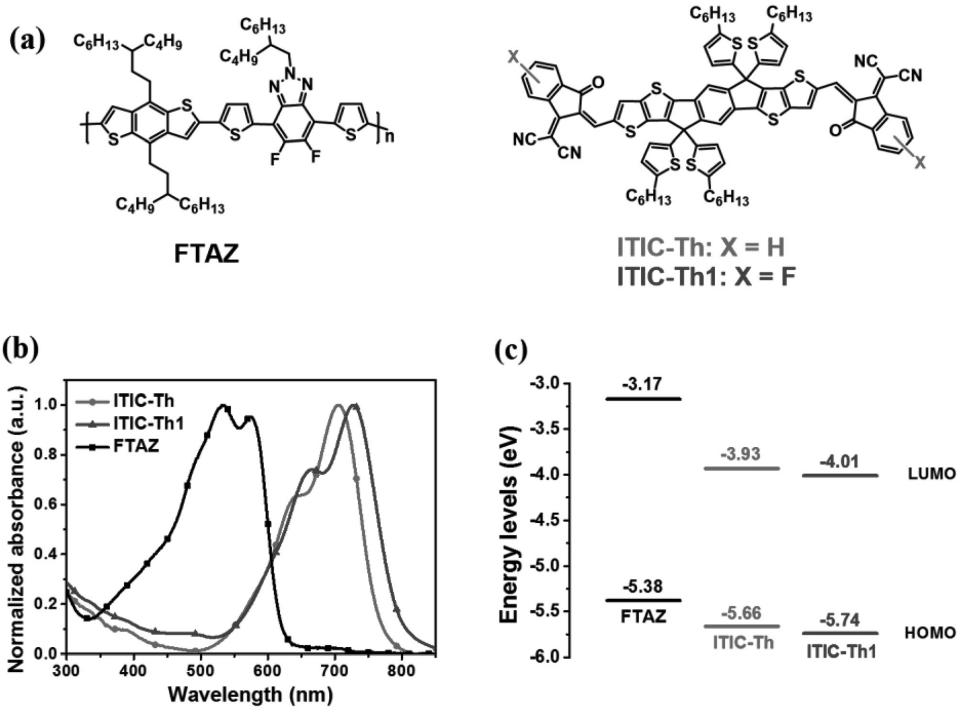

Figure 1. a) Chemical structures of FTAZ, ITIC-Th, and ITIC-Th1. b) UV–vis absorption spectra of FTAZ, ITIC-Th, and ITIC-Th1 in thin film. c) Estimated energy levels of FTAZ, ITIC-Th, and ITIC-Th1 from electrochemical cyclic voltammetry.

open-circuit voltage (V_{OC}), respectively.[11] Some high-performance nonfullerene acceptors have been developed and afforded PCEs as high as 9%, such as perylene diimide and naphthalene diimide small molecules and related polymers.[12–33]

Recently, our group reported a series of fused-ring electron acceptors (FREAs) based on fused-ring electron donor units, such as indacenodithiophene (IDT) and indacenodithieno[3,2-*b*]thiophene (IDTT), flanked with two compact strong electron acceptor units such as 1,1-dicyanomethylene-3-indanone (IC).[34–40] These FREAs such as ITIC (IDTT-IC based electron acceptor),[34] ITIC-Th (IDTT-IC based electron acceptor),[38] and IDIC (IDT-IC based electron acceptor)[37,39] present strong absorption at long wavelength (i.e., small bandgaps) and appropriate energy levels. Moreover, the side chain on the fused-ring donor unit can inhibit the excessive aggregation of the molecules, while the compact acceptor units at the ends retain the strong intermolecular interaction. After blending with some high-performance donors with complementary absorption spectra, the PCEs of FREA-based solar cells achieved over 11%.[41–48] For example, ITIC-Th[38] exhibits a higher electron mobility than its counterpart ITIC with phenyl side chains[34] because the easy polarization of sulfur atom and sulfur–sulfur interaction can enhance the intermolecular interaction. As a result, the PCE of the ITIC-Th-based OSCs was improved to 9.6% when blending with a wide-bandgap polymer PDBT-T1 based on dithienobenzodithiophene and benzodithiophenedione.[38] Later, ITIC-Th was widely used by other groups. For example, Sun and co-workers used ITIC-Th to fabricate ternary blend OSCs, which exhibited a PCE of 10.27%.[49] In another example, Yan and co-workers used ITIC-Th to blend with other polymer donors and got a PCE of 10.88%.[47]

Here, we design and synthesize a new fluorinated ITIC-Th, ITIC-Th1 (**Figure 1**a), by introducing fluorine (F) atoms onto the end-capping group IC. On the one hand, incorporation of F would improve intramolecular interaction, enhance the push–pull effect between the donor unit IDTT and the acceptor unit IC due to the electron-withdrawing effect of F, and finally adjust energy levels and reduce the bandgap, which is beneficial to light harvesting and enhancing J_{SC}. On the other hand, incorporation of F would improve intermolecular interactions through C—F···S, C—F···H, and C—F···π noncovalent interactions and enhance electron mobility, which is beneficial to enhancing J_{SC} and fill factor (FF). Indeed, our results show that fluorinated ITIC-Th1 exhibits redshifted absorption, a smaller optical bandgap and a higher electron mobility than those of nonfluorinated ITIC-Th. Furthermore, nonfullerene OSCs based on fluorinated ITIC-Th1 electron acceptor and a wide-bandgap polymer donor PBnDT-FTAZ (herein abbreviated as FTAZ)[50] (Figure 1a) exhibit PCEs as high as 12.1%, significantly higher than that of the device based on FTAZ and nonfluorinated ITIC-Th (8.88%). The PCE of 12.1% is the highest value in fullerene and nonfullerene-based single-junction binary-blend OSCs. Moreover, the OSCs based on FTAZ:ITIC-Th1 show much better efficiency and stability than the control devices based on FTAZ:$PC_{71}BM$.

Compound ITIC-Th1 was synthesized through facile Knoevenagel condensation reaction between aldehyde 1 and fluorinated IC (2)[51] (Scheme S1, Supporting Information). ITIC-Th1 was fully characterized by spectroscopic methods and elemental analysis (see Supporting Information). ITIC-Th1 exhibits good solubility in common organic solvents (e.g., chloroform, chlorobenzene (CB), and *o*-dichlorobenzene (*o*-DCB))

and good thermal stability (5% weight loss at 271 °C in thermogravimetric analysis, Figure S1, Supporting Information). ITIC-Th1 in dichloromethane solution (10^{-6} M) exhibits strong absorption in the region of 500–750 nm with a maximum extinction coefficient of 1.8×10^5 M^{-1} cm^{-1} at 677 nm (Figure S2, Supporting Information), which is slightly higher than that of ITIC-Th in dichloromethane solution (1.5×10^5 M^{-1} cm^{-1} at 668 nm).[38] From solution to thin film, ITIC-Th1 presents a broader absorption range and the maximum absorption peak shifts from 677 to 728 nm, indicating strong intermolecular interactions among ITIC-Th1 molecules in the solid state (Figure S2, Supporting Information). The absorption of ITIC-Th1 film exhibits an obvious redshift compared with that of ITIC-Th film (Figure 1b), due to enhanced push–pull effect after fluorination. The optical bandgap of ITIC-Th1 estimated from the absorption onset is 1.55, 0.05 eV smaller than that of ITIC-Th, which would benefit harvesting low-energy photons and enhancing J_{SC}. The HOMO (highest occupied molecular orbital) and LUMO (lowest unoccupied molecular orbital) energy levels of ITIC-Th1 film are estimated to be −5.74 and −4.01 eV (Figure 1c), according to the onset oxidation and reduction potentials from electrochemical cyclic voltammetry (Figure S3, Supporting Information), respectively. The HOMO and LUMO of ITIC-Th1 are relatively lower than those of ITIC-Th (HOMO = −5.66 eV; LUMO = −3.93 eV),[38] due to the electron-withdrawing effect of fluorine.

Our previously reported wide-bandgap polymer donor FTAZ exhibits strong absorption at 400–620 nm with a molar extinction coefficient of 9.8×10^4 M^{-1} cm^{-1},[50] which is complementary to the absorption spectra of ITIC-Th and ITIC-Th1 (Figure 1b). Indeed, FTAZ:ITIC-Th (1:1.5, w/w) and FTAZ:ITIC-Th1 (1:1.5, w/w) blended films exhibit broad and strong absorption in 300–800 nm; FTAZ:ITIC-Th1 blend exhibits redshifted and stronger absorption relative to FTAZ:ITIC-Th blend (Figure S4, Supporting Information). The energy levels of FTAZ (HOMO = −5.38 eV; LUMO = −3.17 eV) match with those of ITIC-Th and ITIC-Th1 very well (Figure 1c). FTAZ exhibits a high hole mobility of 1.2×10^{-3} cm^2 V^{-1} s^{-1}.[52] Photoluminescence intensities of pure donor FTAZ and pure acceptor ITIC-Th or ITIC-Th1 are significantly quenched when blending FTAZ with ITIC-Th or ITIC-Th1, suggesting efficient exciton dissociation and charge transfer between FTAZ and ITIC-Th or ITIC-Th1 (Figure S5, Supporting Information). Thus, we used FTAZ as the donor and ITIC-Th or ITIC-Th1 as the acceptor to fabricate bulk heterojunction (BHJ) OSCs with an inverted device structure of indium tin oxide (ITO)/ZnO/FTAZ:acceptor/MoO_x/Ag. We optimized the device fabrication conditions, such as processing solvent, donor/acceptor weight ratio, additive content, and film thickness (Tables S1–S3, Supporting Information). The devices processed with chloroform exhibit higher performance than those processed with CB and *o*-DCB and therefore we choose chloroform as processing solvent (Table S1, Supporting Information). The optimized FTAZ/acceptor weight ratio is 1:1.5, and the optimized content for the processing additive, 1,8-diiodooctane, is 0.25% (v/v) when using chloroform as processing solvent (Table S2, Supporting Information). Changing thickness of the active layer from 80 to 150 nm leads to insignificant variation of PCE from 10% to 12%, while further increasing the thickness leads to significant decrease in PCE; the optimized thickness is 120 nm (Table S3, Supporting Information). The optimized performance parameters are summarized in **Table 1** and the corresponding *J*–*V* curves are shown in **Figure 2**a. The ITIC-Th:FTAZ-based device affords the best PCE of 8.88% with a V_{OC} of 0.915 V, a J_{SC} of 15.84 mA cm^{-2}, and an FF of 61.26%, while the ITIC-Th1:FTAZ-based device achieves the best PCE of 12.1% with a V_{OC} of 0.849 V, a J_{SC} of 19.33 mA cm^{-2}, and an FF of 73.73%. Compared with ITIC-Th, the ITIC-Th1-based devices exhibit a slightly lower V_{OC} but much higher J_{SC} and FF; the lower V_{OC} is mainly due to the deeper LUMO of ITIC-Th1,

Table 1. Best photovoltaic performance of OSCs based on ITIC-Th, ITIC-Th1, and $PC_{71}BM$ via the same fabrication process. The average values and standard deviations of 20 devices are shown in parentheses.

Acceptor	V_{oc} [V]	J_{sc} [mA cm^{-2}]	FF [%]	PCE [%]
ITIC-Th	0.915 (0.914 ± 0.003)	15.84 (15.67 ± 0.23)	61.26 (61.14 ± 0.86)	8.88 (8.67 ± 0.15)
ITIC-Th1	0.849 (0.847 ± 0.002)	19.33 (19.22 ± 0.18)	73.73 (72.56 ± 0.29)	12.1 (11.9 ± 0.1)
$PC_{71}BM$	0.786 (0.785 ± 0.008)	10.20 (10.19 ± 0.23)	65.09 (62.09 ± 1.69)	5.22 (4.97 ± 0.14)

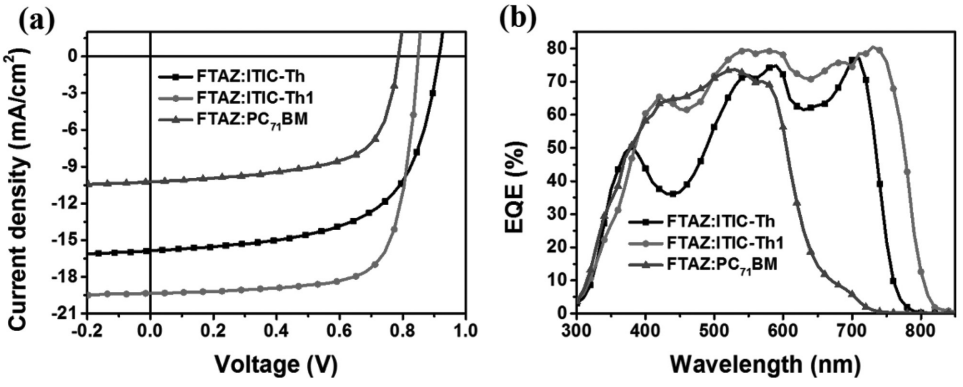

Figure 2. a) Current density versus voltage characteristics. b) EQE curves of the devices based on FTAZ:ITIC-Th, FTAZ:ITIC-Th1, and FTAZ:$PC_{71}BM$ under the same conditions.

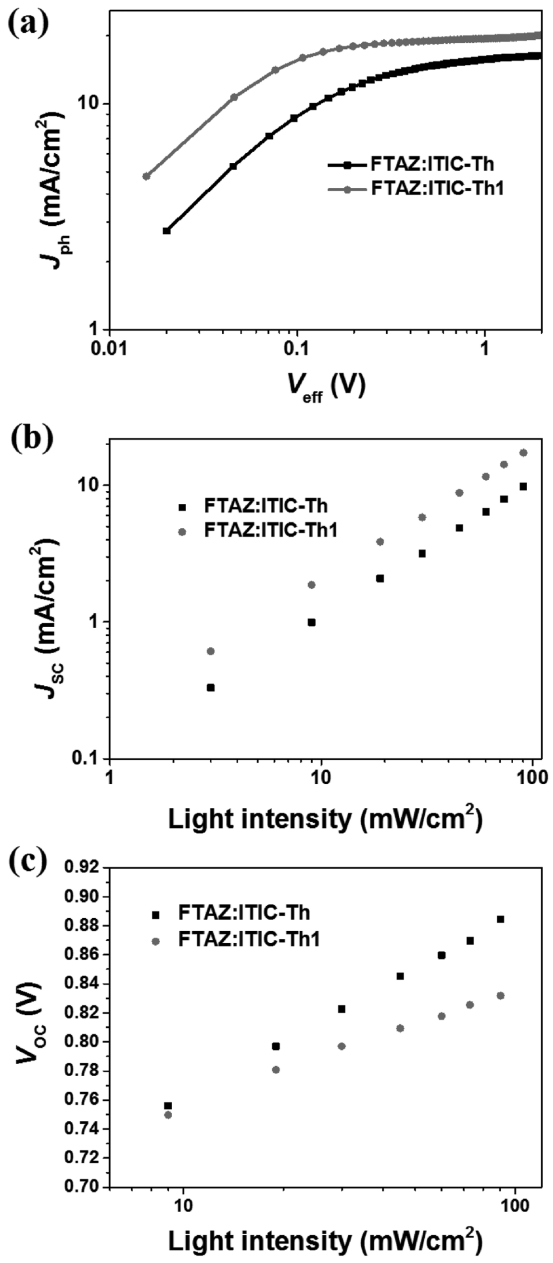

Figure 3. a) Photocurrent density versus effective voltage curves; b) dependence of J_{sc} on light intensity; c) dependence of V_{oc} on light intensity for OSCs based on FTAZ:ITIC-Th and FTAZ:ITIC-Th1.

To investigate carrier recombination in the active layers of ITIC-Th and ITIC-Th1-based cells, J_{sc} was measured as a function of incident light intensity (P_{light}) and the data were fitted to the power law: $J_{sc} \propto P_{light}^{\alpha}$ (Figure 3b).[54] The exponent α for ITIC-Th and ITIC-Th1-based cells is 0.991 and 0.993, respectively, indicating very weak bimolecular recombination at the short circuit condition in the active layers of both devices. We also studied monomolecular recombination via treating V_{oc} as a function of P_{light}. The data were fitted to the linear law: $V_{oc} \propto \mathrm{In}P_{light}$ (Figure 3c).[55] The slope for ITIC-Th and ITIC-Th1-based cell is 1.83 kT/q and 1.36 kT/q, respectively; the smaller slope for ITIC-Th1 cell indicates lower monomolecular recombination.

and good therma
at 271 °C in th
Figure S1, Suppo

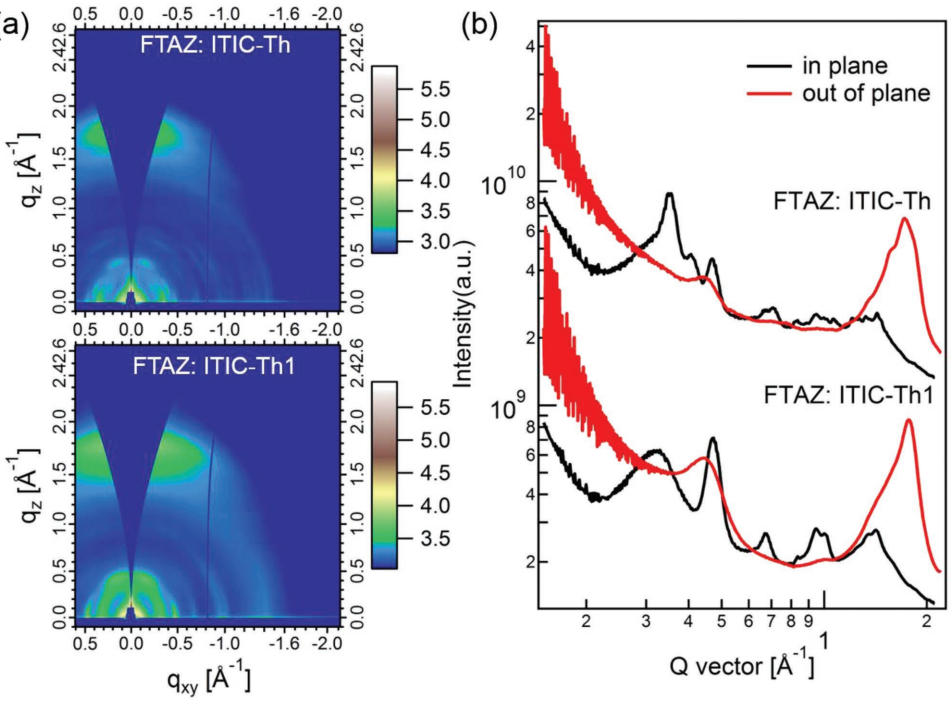

Figure 4. a) 2D GIWAXS patterns and b) scattering profiles of in-plane and out-of-plane for FTAZ:ITIC-Th and FTAZ:ITIC-Th1 blend films.

Space charge limited current method was conducted to obtain electron and hole mobility in the blended films (Figure S9, Supporting Information). The electron mobility of ITIC-Th and ITIC-Th1 in blended films are 4.5×10^{-3} and 7.6×10^{-3} cm^2 V^{-1} s^{-1}, respectively, while the hole mobility of ITIC-Th and ITIC-Th1 blended films are 2.4×10^{-2} and 2.7×10^{-2} cm^2 V^{-1} s^{-1}, respectively. μ_h/μ_e of ITIC-Th and ITIC-Th1 blends are 5.3 and 3.5, respectively. The higher hole/electron mobility and more balanced charge transport in FTAZ:ITIC-Th1 blended film are responsible for its higher J_{sc} and higher FF. The above exciton/charge dynamics data imply that both ITIC-Th and ITIC-Th1-based OSCs exhibit good charge extraction and very weak bimolecular recombination. However, the ITIC-Th1-based cells exhibit better exciton generation and dissociation, less monomolecular recombination, and faster and more balanced hole/electron transport than the ITIC-Th counterpart, thus contributing to higher J_{sc} and high FF.

The morphology of the active layer based on ITIC-Th1 and ITIC-Th was studied by atomic force microscopy (AFM), transmission electron microscopy (TEM), grazing-incidence wide-angle X-ray scattering (GIWAXS), and resonant soft X-ray scattering (RSoXS). In the AFM images (Figure S10, Supporting Information), the root-mean-square roughness of FTAZ:ITIC-Th and FTAZ:ITIC-Th1 films is 4.32 and 7.69 nm, respectively. In the phase images, both films exhibit uniform nanoscale aggregation domains. In the TEM images (Figure S11, Supporting Information), the FTAZ:ITIC-Th1 blended film presents finer and clearer aggregation domains than the FTAZ:ITIC-Th blended film.

GIWAXS is used to investigate the molecular packing of FTAZ:ITIC-Th and FTAZ:ITIC-Th1. The π–π stacking peaks of ITIC-Th and ITIC-Th1 are located at ≈1.8 Å. As shown in **Figure 4**, it is obvious that almost all the peaks are stronger/sharper for FTAZ:ITIC-Th1, indicating the enhanced molecular packing in FTAZ:ITIC-Th1 films. The coherence length of ITIC-Th and ITIC-Th1 π–π stacking is calculated (via the Scherrer equation)[56] to be 3.7 and 4.0 nm, respectively. The improved molecular packing is known to benefit the charge transport. Thus, FTAZ:ITIC-Th1 shows higher mobility, which leads to higher FF and thus higher PCE.

Resonant soft X-ray scattering (R-SoXS) is also employed to obtain the phase separation information of FTAZ:ITIC-Th and FTAZ:ITIC-Th1 blend films (**Figure 5**).[57] The photon energy of 284.8 eV is selected to obtain enhanced material contrast. The

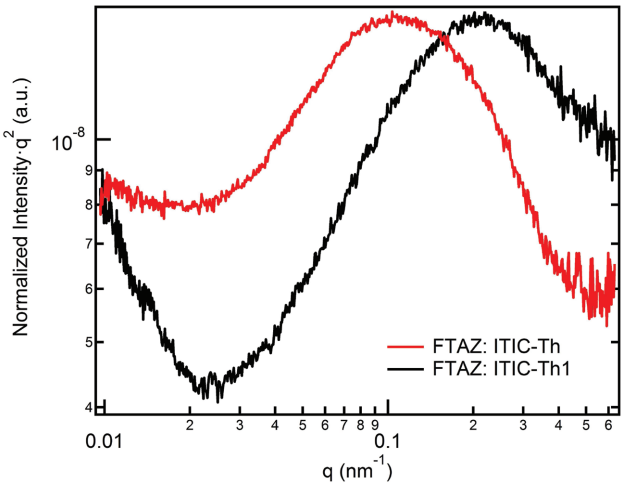

Figure 5. Normalized R-SoXS profiles in log scale for FTAZ:ITIC-Th and ITIC-Th1 blend films.

mode of the distribution s_{mode} of the scattering corresponds to the characteristic mode length scale, ξ. It is noted that the mode domain size is the half of ξ. The mode domain size of FTAZ:ITIC-Th and FTAZ:ITIC-Th1 is calculated to be 29 and 15 nm, respectively. These results are consistent with the TEM results. Due to the limited exciton diffusion length (10–20 nm), smaller domains are favorable for the charge separation. Therefore, FTAZ: ITIC-Th1 shows higher J_{SC}.

In summary, we designed and synthesized a fluorinated FREA, ITIC-Th1. Compared with the nonfluorinated counterpart ITIC-Th, ITIC-Th1 presents a slightly deeper LUMO, redshifted absorption, and a smaller bandgap. FTAZ:ITIC-Th1 BHJ films exhibit stronger molecular packing and longer coherence length, leading to higher electron and hole yet balanced mobilities. Moreover, FTAZ:ITIC-Th1 films present smaller domain sizes to afford more D/A interfaces for exciton dissociation and reduce monomolecular recombination. As a result, nonfullerene OSCs based on FTAZ:ITIC-Th1 exhibit PCEs as high as 12.1%, significantly higher than those of BHJ devices based on FTAZ:nonfluorinated ITIC-Th (8.88%) and FTAZ:$PC_{71}BM$ (5.22%). The PCE of 12.1% is among the highest values in fullerene and nonfullerene-based single-junction OSCs. Moreover, the nonfullerene OSCs show better thermal stability than the $PC_{71}BM$-based control devices. Our results demonstrate that the fluorinated acceptor ITIC-Th1 is very promising for high-performance OSCs.

Supporting Information

Supporting Information is available from the Wiley Online Library or from the author.

Acknowledgements

X.Z. thanks the 973 Program (Grant No. 2013CB834702) and the National Natural Science Foundation of China (Grant No. 91433114). Q.Z. and W.Y. were supported by the Office of Naval Research (Grant No. N000141410221) and National Science Foundation (Grant No. DMR-1507249). W.M. thanks for the support from Ministry of Science and Technology (Grant No. 2016YFA0200700) and NSFC (Grant Nos. 21504066 and 21534003). X-ray data were acquired at beamlines 7.3.3 and 11.0.1.2 at the Advanced Light Source, which was supported by the Director, Office of Science, Office of Basic Energy Sciences, of the U.S. Department of Energy under Contract No. DE-AC02-05CH11231. The authors thank Chenhui Zhu at beamline 7.3.3 and Cheng Wang at beamline 11.0.1.2 for assistance with data acquisition.

Received: January 8, 2017
Revised: February 8, 2017
Published online: March 10, 2017

[1] G. Li, R. Zhu, Y. Yang, *Nat. Photonics* **2012**, *6*, 153.
[2] Y.-J. Cheng, S.-H. Yang, C.-S. Hsu, *Chem. Rev.* **2009**, *109*, 5868.
[3] L. Lu, T. Zheng, Q. Wu, A. M. Schneider, D. Zhao, L. Yu, *Chem. Rev.* **2015**, *115*, 12666.
[4] J. Wang, K. Liu, L. Ma, X. Zhan, *Chem. Rev.* **2016**, *116*, 14675.
[5] Y. Lin, Y. Li, X. Zhan, *Chem. Soc. Rev.* **2012**, *41*, 4245.
[6] F. C. Krebs, N. Espinosa, M. Hösel, R. R. Søndergaard, M. Jørgensen, *Adv. Mater.* **2014**, *26*, 29.
[7] a) Y. He, Y. Li, *Phys. Chem. Chem. Phys.* **2011**, *13*, 1970; b) C. Zhang, S. Chen, Z. Xiao, Q. Zuo, L. Ding, *Org. Lett.* **2012**, *14*, 1508.
[8] a) J. E. Anthony, A. Facchetti, M. Heeney, S. R. Marder, X. Zhan, *Adv. Mater.* **2010**, *22*, 3876; b) D. He, X. Du, Z. Xiao, L. Ding, *Org. Lett.* **2014**, *16*, 612; c) Z. Xiao, X. Geng, D. He, X. Jia, L. Ding, *Energy Environ. Sci.* **2016**, *9*, 2114.
[9] J. Zhao, Y. Li, G. Yang, K. Jiang, H. Lin, H. Ade, W. Ma, H. Yan, *Nat. Energy* **2016**, *1*, 15027.
[10] M. Li, K. Gao, X. Wan, Q. Zhang, B. Kan, R. Xia, F. Liu, X. Yang, H. Feng, W. Ni, Y. Wang, J. Peng, H. Zhang, Z. Liang, H.-L. Yip, X. Peng, Y. Cao, Y. Chen, *Nat. Photonics* **2017**, *11*, 85.
[11] Y. Lin, X. Zhan, *Mater. Horiz.* **2014**, *1*, 470.
[12] X. Zhan, Z. Tan, B. Domercq, Z. An, X. Zhang, S. Barlow, Y. Li, D. Zhu, B. Kippelen, S. R. Marder, *J. Am. Chem. Soc.* **2007**, *129*, 7246.
[13] X. Zhan, A. Facchetti, S. Barlow, T. J. Marks, M. A. Ratner, M. R. Wasielewski, S. R. Marder, *Adv. Mater.* **2011**, *23*, 268.
[14] E. Zhou, J. Cong, K. Hashimoto, K. Tajima, *Adv. Mater.* **2013**, *25*, 6991.
[15] X. Zhang, Z. Lu, L. Ye, C. Zhan, J. Hou, S. Zhang, B. Jiang, Y. Zhao, J. Huang, S. Zhang, Y. Liu, Q. Shi, Y. Liu, J. Yao, *Adv. Mater.* **2013**, *25*, 5791.
[16] T. Earmme, Y.-J. Hwang, N. M. Murari, S. Subramaniyan, S. A. Jenekhe, *J. Am. Chem. Soc.* **2013**, *135*, 14960.
[17] H. Li, F. S. Kim, G. Ren, E. C. Hollenbeck, S. Subramaniyan, S. A. Jenekhe, *Angew. Chem., Int. Ed.* **2013**, *52*, 5513.
[18] Y. Lin, Y. Wang, J. Wang, J. Hou, Y. Li, D. Zhu, X. Zhan, *Adv. Mater.* **2014**, *26*, 5137.
[19] R. Shivanna, S. Shoaee, S. Dimitrov, S. K. Kandappa, S. Rajaram, J. R. Durrant, K. S. Narayan, *Energy Environ. Sci.* **2014**, *7*, 435.
[20] P. E. Hartnett, A. Timalsina, H. S. Matte, N. Zhou, X. Guo, W. Zhao, A. Facchetti, R. P. Chang, M. C. Hersam, M. R. Wasielewski, T. J. Marks, *J. Am. Chem. Soc.* **2014**, *136*, 16345.
[21] X. Guo, A. Facchetti, T. J. Marks, *Chem. Rev.* **2014**, *114*, 8943.
[22] Y. Zhong, M. T. Trinh, R. Chen, W. Wang, P. P. Khlyabich, B. Kumar, Q. Xu, C.-Y. Nam, M. Y. Sfeir, C. Black, M. L. Steigerwald, Y.-L. Loo, S. Xiao, F. Ng, X. Y. Zhu, C. Nuckolls, *J. Am. Chem. Soc.* **2014**, *136*, 15215.
[23] Y. Zhong, M. T. Trinh, R. Chen, G. E. Purdum, P. P. Khlyabich, M. Sezen, S. Oh, H. Zhu, B. Fowler, B. Zhang, W. Wang, C. Y. Nam, M. Y. Sfeir, C. T. Black, M. L. Steigerwald, Y. L. Loo, F. Ng, X. Y. Zhu, C. Nuckolls, *Nat. Commun.* **2015**, *6*, 8242.
[24] H. Li, Y.-J. Hwang, B. A. E. Courtright, F. N. Eberle, S. Subramaniyan, S. A. Jenekhe, *Adv. Mater.* **2015**, *27*, 3266.
[25] D. Sun, D. Meng, Y. Cai, B. Fan, Y. Li, W. Jiang, L. Huo, Y. Sun, Z. Wang, *J. Am. Chem. Soc.* **2015**, *137*, 11156.
[26] Q. Wu, D. Zhao, A. M. Schneider, W. Chen, L. Yu, *J. Am. Chem. Soc.* **2016**, *138*, 7248.
[27] Y. Liu, C. Mu, K. Jiang, J. Zhao, Y. Li, L. Zhang, Z. Li, J. Y. Lai, H. Hu, T. Ma, R. Hu, D. Yu, X. Huang, B. Z. Tang, H. Yan, *Adv. Mater.* **2015**, *27*, 1015.
[28] D. Meng, H. Fu, C. Xiao, X. Meng, T. Winands, W. Ma, W. Wei, B. Fan, L. Huo, N. L. Doltsinis, Y. Li, Y. Sun, Z. Wang, *J. Am. Chem. Soc.* **2016**, *138*, 10184.
[29] H. Zhong, C.-H. Wu, C.-Z. Li, J. Carpenter, C.-C. Chueh, J.-Y. Chen, H. Ade, A. K. Y. Jen, *Adv. Mater.* **2016**, *28*, 951.
[30] J. Liu, S. Chen, D. Qian, B. Gautam, G. Yang, J. Zhao, J. Bergqvist, F. Zhang, W. Ma, H. Ade, O. Inganäs, K. Gundogdu, F. Gao, H. Yan, *Nat. Energy* **2016**, *1*, 16089.
[31] Y. Guo, Y. Li, O. Awartani, J. Zhao, H. Han, H. Ade, D. Zhao, H. Yan, *Adv. Mater.* **2016**, *28*, 8483.
[32] L. Gao, Z. G. Zhang, L. Xue, J. Min, J. Zhang, Z. Wei, Y. Li, *Adv. Mater.* **2016**, *28*, 1884.
[33] C. Dou, X. Long, Z. Ding, Z. Xie, J. Liu, L. Wang, *Angew. Chem., Int. Ed.* **2016**, *55*, 1436.

[34] Y. Lin, J. Wang, Z. G. Zhang, H. Bai, Y. Li, D. Zhu, X. Zhan, *Adv. Mater.* **2015**, *27*, 1170.
[35] Y. Lin, Z. G. Zhang, H. Bai, J. Wang, Y. Yao, Y. Li, D. Zhu, X. Zhan, *Energy Environ. Sci.* **2015**, *8*, 610.
[36] Y. Wu, H. Bai, Z. Wang, P. Cheng, S. Zhu, Y. Wang, W. Ma, X. Zhan, *Energy Environ. Sci.* **2015**, *8*, 3215.
[37] Y. Lin, Q. He, F. Zhao, L. Huo, J. Mai, X. Lu, C. J. Su, T. Li, J. Wang, J. Zhu, Y. Sun, C. Wang, X. Zhan, *J. Am. Chem. Soc.* **2016**, *138*, 2973.
[38] Y. Lin, F. Zhao, Q. He, L. Huo, Y. Wu, T. C. Parker, W. Ma, Y. Sun, C. Wang, D. Zhu, A. J. Heeger, S. R. Marder, X. Zhan, *J. Am. Chem. Soc.* **2016**, *138*, 4955.
[39] Y. Lin, F. Zhao, Y. Wu, K. Chen, Y. Xia, G. Li, S. K. Prasad, J. Zhu, L. Huo, H. Bin, Z. G. Zhang, X. Guo, M. Zhang, Y. Sun, F. Gao, Z. Wei, W. Ma, C. Wang, J. Hodgkiss, Z. Bo, O. Inganas, Y. Li, X. Zhan, *Adv. Mater.* **2017**, *29*, 1604155.
[40] P. Cheng, M. Zhang, T. Lau, Y. Wu, B. Jia, J. Wang, C. Yan, M. Qin, X. Lu, X. Zhan, *Adv. Mater.* **2017**, *29*, 1605216.
[41] W. Zhao, D. Qian, S. Zhang, S. Li, O. Inganäs, F. Gao, J. Hou, *Adv. Mater.* **2016**, *28*, 4734.
[42] H. Bin, Z. G. Zhang, L. Gao, S. Chen, L. Zhong, L. Xue, C. Yang, Y. Li, *J. Am. Chem. Soc.* **2016**, *138*, 4657.
[43] H. Bin, L. Gao, Z. G. Zhang, Y. Yang, Y. Zhang, C. Zhang, S. Chen, L. Xue, C. Yang, M. Xiao, Y. Li, *Nat. Commun.* **2016**, *7*, 13651.
[44] Y. Yang, Z. G. Zhang, H. Bin, S. Chen, L. Gao, L. Xue, C. Yang, Y. Li, *J. Am. Chem. Soc.* **2016**, *138*, 15011.
[45] S. Li, L. Ye, W. Zhao, S. Zhang, S. Mukherjee, H. Ade, J. Hou, *Adv. Mater.* **2016**, *28*, 9423.
[46] H. Yao, Y. Chen, Y. Qin, R. Yu, Y. Cui, B. Yang, S. Li, K. Zhang, J. Hou, *Adv. Mater.* **2016**, *28*, 8283.
[47] Z. Li, K. Jiang, G. Yang, J. Y. Lai, T. Ma, J. Zhao, W. Ma, H. Yan, *Nat. Commun.* **2016**, *7*, 13094.
[48] D. Baran, R. S. Ashraf, D. A. Hanifi, M. Abdelsamie, N. Gasparini, J. A. Rohr, S. Holliday, A. Wadsworth, S. Lockett, M. Neophytou, C. J. M. Emmott, J. Nelson, C. J. Brabec, A. Amassian, A. Salleo, T. Kirchartz, J. R. Durrant, I. McCulloch, *Nat. Mater.* **2017**, *16*, 363.
[49] T. Liu, Y. Guo, Y. Yi, L. Huo, X. Xue, X. Sun, H. Fu, W. Xiong, D. Meng, Z. Wang, F. Liu, T. P. Russell, Y. Sun, *Adv. Mater.* **2016**, *28*, 10008.
[50] S. C. Price, A. C. Stuart, L. Yang, H. Zhou, W. You, *J. Am. Chem. Soc.* **2011**, *133*, 4625.
[51] S. Dai, F. Zhao, Q. Zhang, T. Lau, T. Li, K. Liu, Q. Ling, C. Wang, X. Lu, W. You, X. Zhan, *J. Am. Chem. Soc.* **2017**, *139*, 1336.
[52] W. Li, S. Albrecht, L. Yang, S. Roland, J. R. Tumbleston, T. McAfee, L. Yan, M. A. Kelly, H. Ade, D. Neher, W. You, *J. Am. Chem. Soc.* **2014**, *136*, 15566.
[53] V. Mihailetchi, L. Koster, J. Hummelen, P. Blom, *Phys. Rev. Lett.* **2004**, *93*, 216601.
[54] I. Riedel, J. Parisi, V. Dyakonov, L. Lutsen, D. Vanderzande, J. C. Hummelen, *Adv. Funct. Mater.* **2004**, *14*, 38.
[55] L. J. A. Koster, V. D. Mihailetchi, R. Ramaker, P. W. Blom, *Appl. Phys. Lett.* **2005**, *87*, 123509.
[56] D.-M. Smilgies, *J. Appl. Cryst.* **2013**, *46*, 286.
[57] E. Gann, A. T. Young, B. A. Collins, H. Yan, J. Nasiatka, H. A. Padmore, H. Ade, A. Hexemer, C. Wang, *Rev. Sci. Instrum.* **2012**, *83*, 045110.